ANNUAL REPORT FOR SCEC AWARD #16096

Submitted 15 March 2017

Depth Dependent In Situ Crustal Stress Models With Implications For Fault Strength In Southern California

Investigators: Karen Luttrell (LSU), Bridget Smith-Konter (UH)

I. PROJECT OVERVIEW

A. Abstract

We have extended our previous models of *in situ* crustal stress, with orientation derived from inverted focal mechanisms and a magnitude estimated as that required to overcome resistance from topography, to include depth dependence from topography, and have created a framework for including 4-D fault loading stress over several earthquake cycles. The preliminary results indicate stress increases with depth, as expected, to a maximum in the seismogenic zone of ~62 MPa differential stress in the areas of most rugged topography. We have also developed a framework to resolve a given stress field onto Community Fault Model planes to estimate sustained normal and shear stress magnitude. These results can be used to investigate variations in fault strength with depth and throughout the plate boundary system. The code for conducting this analysis will be made available to the SCEC community as part of the new CXM modeling efforts. Finally, we have investigated prospects for extending direct observations of stress state from boreholes, by searching through ~2500 historic industry-collected well logs from California, from a proprietary database accessible by students at Louisiana State University. From the available logs, we identified one with information from oriented logging tools that could be used to ascertain stress azimuth, and subsequently continued our analysis of stress orientations indicated by different observation techniques.

B. SCEC Annual Science Highlights

Stress and Deformation Through Time (SDOT)
Tectonic Geodesy
Communication, Education, and Outreach

C. Exemplary Figure

Figure 2: a) minimum magnitude () of stress field required to overcome the load of topography in the crust, at 5 km depth. This metric is equivalent to the maximum shear stress on an optimally oriented plane, for a given stress tensor. b) maximum shear stress from depth dependent minimum stress field estimate resolved onto the planes of the Community Fault Model [*Plesch et al*., 2007; *Nicholson et al*., 2013]. Each point represents the centroid of a CFM fault patch triangle c) same as b), focused on the SAF, SJF, and Banning segments (black box in b). d) 3-D view of region shown in c). Note the depth dependence of resolved stress estimates on various fault segments.

D. SCEC Science Priorities

2d. Development of a Community Stress Model (CSM) for Southern California, based on merging information from borehole measurements, focal mechanisms, paleo-slip indicators, observations of damage, topographic loading, geodynamic and earthquake-cycle modeling, and induced seismicity.

1b. Focused laboratory, numerical, and geophysical studies of the character of the lower crust, its rheology, stress state, and expression in surface deformation.

E. Intellectual Merit

These findings directly support an important objective of SCEC and the CSM, to synthesize the insights offered by diverse contributed models in order to gain a more holistic understanding of the 4D stress field and be better situated to present a community-endorsed stress model to the broader SCEC community. Our investigations have developed novel estimates of stress magnitude and established novel techniques to infer the near-fault character of the tectonic driving stress and explore the relative importance of locked faults on the *in situ* stress state.

F. Broader Impacts

This project has enabled one LSU undergraduate student to conduct research on southern California stress state and gain valuable experience in data mining, computer programming, figure preparation, and writing skills. This research was presented at the 2016 SCEC Annual Meeting.

G. Project Publications

Peer reviewed publications and manuscripts in preparation

Luttrell, K., and B. Smith-Konter (2017a), Limits on crustal differential stress in southern California from topography and earthquake focal mechanisms, *Geophys. J. Int.*, *in review*.

Luttrell, K., and B. Smith-Konter (2017b), Near fault crustal stress in southern California with implications for heterogeneous tectonic loading, *manuscript in preparation*.

Invited and Contributed Conference Presentations

(Student authors underlined, * indicates invited presentations)

Luttrell, K., and B. Smith-Konter (2016), Regional-Scale Models of Crustal Stress Along the Pacific-North America Plate Boundary, with Implications for Heterogeneous Tectonic Loading and In Situ Stress Magnitude, GSA South-Central Section Meeting, Abstract #273845.

Luttrell, K., and B. Smith-Konter (2016), Regional-Scale Models of Crustal Stress in Southern California, with Implications for Heterogeneous Tectonic Loading and In Situ Stress Magnitude, SSA Annual Meeting, Abstract 16-698.

*Luttrell, K (2016), Crustal stress along the San Andreas fault system: Insights from a community of stress models, Colloquium, Department of Earth and Planetary Sciences, Harvard University, April 2016.

*Luttrell, K (2016), How stressed are we really? Harnessing community models to characterize the crustal stress field in southern California, Invited Plenary Speaker, Session 3: Modeling Fault Systems – Community Models, SCEC Annual Meeting.

II. TECHNICAL REPORT

1. SUMMARY OF MAJOR FINDINGS

The goal of this research has been to extend our previously developed single-depth model representations of *in situ* stress to estimate the 4-D stress field throughout the crust, with the application of refining estimates of the strength of faults in the region. In the process, we make use of both direct and indirect indications of static stress state, and have worked toward expanding the catalog of available direct observations. Three primary findings have resulted from 2016 SCEC Award #16096, and form the basis of several avenues of future research.

- We have extended our models of *in situ* crustal stress, with orientation derived from inverted focal mechanisms and a magnitude estimated as that required to overcome resistance from topography [*Luttrell and Smith-Konter*, 2017], to include depth dependence from topography, and have created a framework for including 4-D fault loading stress over several earthquake cycles. The preliminary results indicate stress increases with depth, as expected, to a maximum in the seismogenic zone of ~62 MPa differential stress in the areas of most rugged topography.
- We have developed a framework to resolve a given stress field onto Community Fault Model planes to estimate sustained normal and shear stress magnitude. These results can be used to investigate variations in fault strength with depth and throughout the plate boundary system. The code for conducting this analysis will be made available to the SCEC community as part of the new CXM modeling efforts.
- We have investigated prospects for extending direct observations of stress state from boreholes, by searching through ~2500 historic industry-collected well logs from California, from a proprietary database accessible by students at Louisiana State University. From the available logs, we identified one with information from oriented logging tools that could be used to ascertain stress azimuth, and have subsequently continued our analysis of stress orientations indicated by different observation techniques.

These findings directly support an important objective of SCEC and the CSM, to synthesize the insights offered by diverse contributed models in order to gain a more holistic understanding of the 4-D stress field and be better situated to present a community-endorsed stress model to the broader SCEC community. Funding from this award enabled one LSU undergraduate (Phoenix Harris) to conduct summer research on southern California stress state, primarily by searching through available historic well logs in California.

This work was presented in talks at 2016 South Central GSA meeting and the 2016 SSA meeting, and as an invited colloquium at Harvard University in the Spring of 2016. It was also presented in an invited plenary talk at the 2016 SCEC Annual Meeting. It has contributed to preparation of a manuscript in review at *Geophysical Journal International* [*Luttrell and Smith-Konter*, 2017], and in a second mature manuscript to be submitted for publication in *Journal of Geophysical Research* [*Luttrell and Smith-Konter*, 2017, manuscript in preparation].

2. CHARACTERIZING IN SITU STRESS THROUGHOUT THE UPPER CRUST

Direct observations of *in situ* stress are rare, owing to the difficulty of making such measurements [*Zoback et al*., 2010]. Those observations that are available principally come from drilling for scientific or industrial purposes [e.g., *Zoback and Healy*, 1992; *Brudy et al*., 1997; *Wilde and Stock*, 1997; *Zajac and Stock*, 1997; *Hickman and Zoback*, 2004]. However, such observations are limited to locations where boreholes are present and where data have been made publically available. Alternatively, several indirect observations can be used to constrain properties of the stress field. Groups of earthquake focal mechanisms can be inverted to infer the orientation of the *in situ* stress field (**Q**) [*Hardebeck and Michael*, 2006; *Yang et al*., 2012; *Yang and Hauksson*, 2013] but cannot constrain stress magnitude. The rate of stress accumulation on major locked fault segments (**L**) is well constrained by surface geodesy, though the magnitude of this stress depends on both the loading time and the degree to which the most recent rupture achieved complete stress drop [*Smith-Konter and Sandwell*, 2009; *Tong et al*., 2013]. Crustal stress variations due to topography (**T**) can be calculated, with constraints from gravity observations, providing one of the few true magnitude estimates of considered processes [*Luttrell and Sandwell*, 2012; *Luttrell and Smith-Konter*, 2017].

Because the load of topography by itself creates a stress field that is, in general, in opposition to the orientation of the *in situ* stress, the two stress fields (**T** and **Q**) can be balanced against one another to estimate the magnitude of *in situ* stress ($\Delta\sigma$) required to maintain *in situ* orientation **Q** in the presence of **T**. In order to determine the total stress magnitude in this way, two further assumptions must be made about the nature of the tectonic stress field. First, we must assume that the load of topography is not the dominant source of stress in southern California. Second, we assume that, relative to the influence of topography, the "other" sources of stress, not including topography (e.g., far-field tectonic plate driving stresses and local stress accumulation on locked faults) are dominant over the study region, such that the orientation of the total stress field is approximately aligned with the orientation of these non-topographic sources of stress. This is equivalent to assuming that the stress contributions from topography are approximately negligible in determining the overall character of the stress field across southern California.

We calculate stress from topography by assuming topography has been built to a state of near critical failure in an elastic-perfectly-plastic crust [e.g., *Dahlen*, 1990], such that the ruggedness of topography is itself an indicator of the stress being supported within the crust. This crustal stress field is calculated semianalytically, convolving a Green's function for non-identical point normal tractions at the surface and base of a uniform elastic plate with both the surface topography and the buoyant load of topography at the Moho, determined by comparing the gravity in the area with that predicted from a crust with varying effective elastic thickness. (Wavelengths longer than $2\pi h$, where h is the crustal thickness, are excluded, as these features are dominantly supported by isostasy in the mantle rather than by stress variations within the crust.) The resulting calculation is fully depth dependent and 3-dimensional.

We add this stress field **T** to the stress field with orientation from earthquake focal mechanism inversion **Q** [*Yang and Hauksson*, 2013] scaled by the variable differential stress estimate ($\Delta\sigma$), and determine the 3D variation of the minimum magnitude sufficient to ensure the total stress field aligns with the observed focal mechanisms.

Figure 1 summarizes these results by detailing the fraction of the model region able to be satisfactorily fit by a stress field with magnitude $\Delta\sigma$, over depths from the surface through the upper crust (to 15 km depth). The preliminary results indicate stress increases with depth, as expected, to a maximum in the seismogenic zone of ~62 MPa differential stress in the areas of most rugged topography. (Figure 2a demonstrates the lateral variation of $\Delta\sigma/2$ for a single depth of 5 km). Closer to the surface, in areas better represented by stress observations from scientific drilling than by those from earthquake focal mechanisms, the areas of most rugged topography can be maintained with a differential stress closer to 30 MPa.

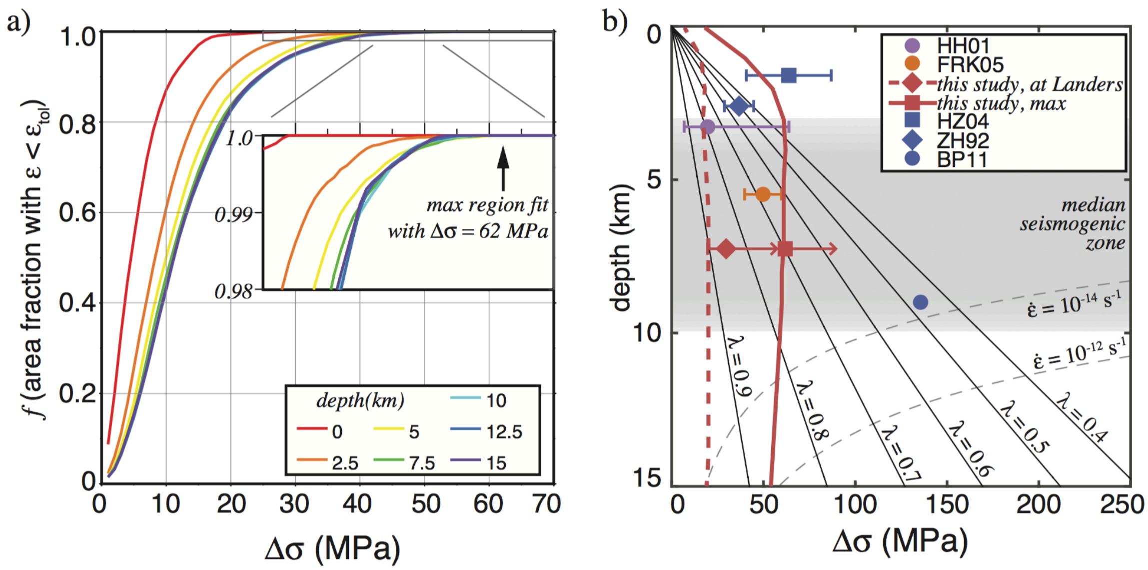

Figure 1: Depth dependent estimates of differential stress. a) fraction of model region fit within tolerance as a function of differential stress magnitude at depth indicated. Inset figure is zoom of $f >$ 0.98 region. b) brittle yield strength in the upper crust for coefficient of friction (μ_f) 0.6, with varying ratios of pore pressure to hydrostatic pressure (λ) as indicated. Dashed gray lines represent ductile yield strength for given strain rate [e.g., *Hirth et al*., 2001]. Symbols indicate estimates of differential stress from previous studies: HH01 [*Hardebeck and Hauksson*, 2001]; FRK05 [*Fialko et al*., 2005]; HZ04 [*Hickman and Zoback*, 2004]; ZH92 [*Zoback and Healy*, 1992]; BP11 [*Behr and Platt*, 2011]. Depth dependent differential stress values from this study are indicated by red symbols. Median seismogenic depths [*Hauksson et al*., 2012] indicated as gray shaded region. After *Luttrell and Smith-Konter* [2017].

Differential stress magnitude is expected to vary with depth following the yield strength envelope of crustal material [e.g., *Brace and Kohlstedt*, 1980]. Figure 1b demonstrates this dependence and illustrates the estimate obtained from this study along with complimentary estimates of differential stress magnitude at depth in southern California. The solid red line indicates the highest minimum differential stress required to support topography across the entire region, while the dashed line represents the stress required specifically in the region of the 1992 M7.3 Landers earthquake, which provided estimates of *in situ* differential stress based on observed rotations of the stress field caused by the rupture [*Hardebeck and Hauksson*, 2001]. Overall, the estimates of differential stress from this study are generally consistent with estimates from these complimentary methods.

3. Resolving 3-D Stress Fields onto the SCEC Community Fault Model

The estimates of differential stress $(\sigma_1 - \sigma_3)$ presented above represent twice the maximum possible shear stress that could be resolved in an optimal direction on an optimally oriented plane at any point throughout the model region $(\sigma_1 - \sigma_3)/2$. Figure 2a shows the maximum possible shear stress on an optimally oriented fault plane at a depth of 5 km, near the top of the median seismogenic zone. Spatial variations in the magnitude of maximum shear stress are clear, with higher shear stresses potentially required in the regions of most rugged topography. However, we are particularly interested in how this general stress field translates into shear and normal stresses resolved onto the particular fault planes in the region.

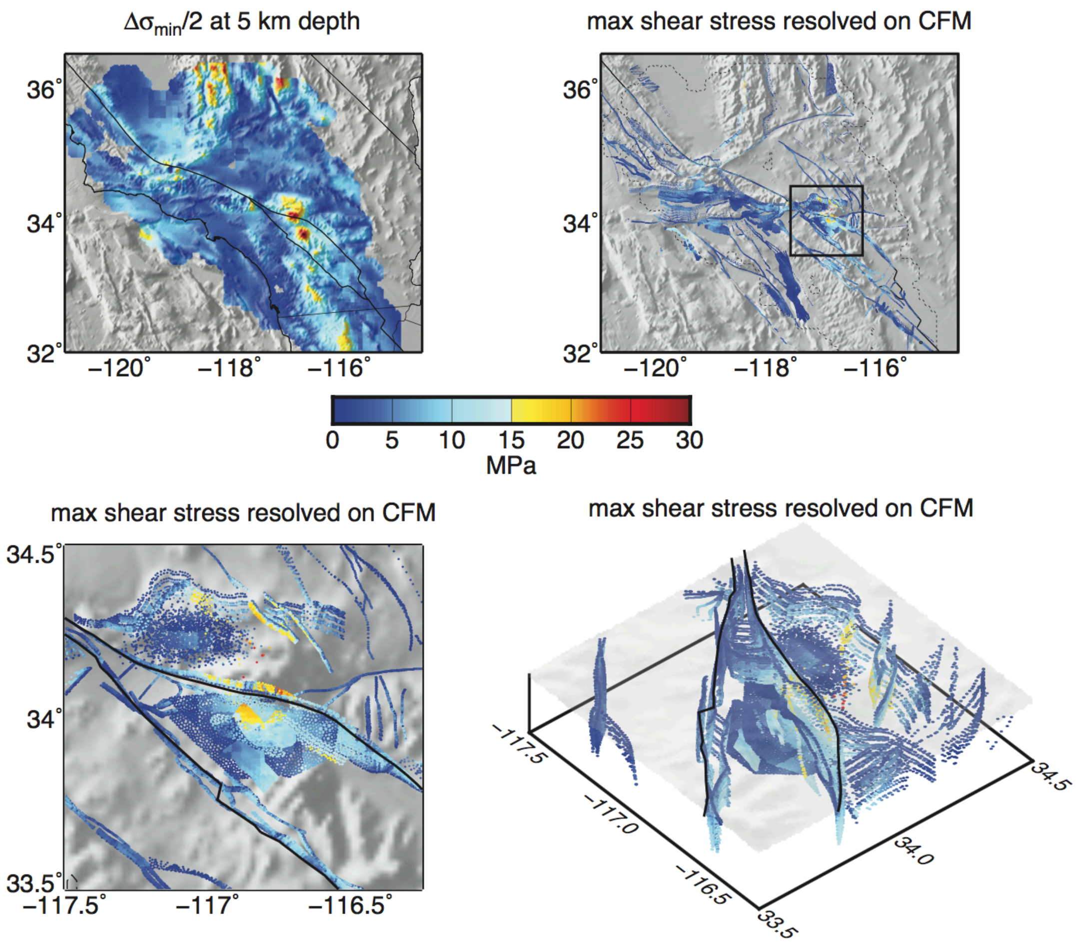

Figure 2: a) minimum magnitude (Δσ/2) of stress field required to overcome the load of topography in the crust, at 5 km depth. This metric is equivalent to the maximum shear stress on an optimally oriented plane, for a given stress tensor. b) maximum shear stress from depth dependent minimum stress field estimate resolved onto the planes of the Community Fault Model [*Plesch et al.*, 2007; *Nicholson et al.*, 2013]. Each point represents the centroid of a CFM fault patch triangle c) same as b), focused on the SAF, SJF, and Banning segments (black box in b). d) 3-D view of region shown in c). Note the depth dependence of resolved stress estimates on various fault segments.

To answer this question, we developed a series of computational scripts, written in the widely-used language of MATLAB, to resolve any arbitrary 3-D stress field onto the ~161,000 individual fault patch elements that make up the ~300 fault segments included in the SCEC Community Fault Model (version 5, as released in 2014) [*Plesch et al*., 2007; *Nicholson et al*., 2013]. As demonstrated in Figure 2, this allows us a powerful tool visualize stress fields at depth, and to check that modeled stress fields reproduce "real world behavior" on actual fault planes. This is a function that has often been requested by users of the Community Stress Model at workshops throughout SCEC4. These scripts represent simple portable utilities that can be shared with the SCEC Community, particularly as part of the new CXM modeling efforts in SCEC5.

4. In Situ Observations of Stress Field Orientation

Award support has also been used to support LSU Undergraduate Research Assistant Phoenix Harris in Summer 2016 to examine well logs collected by various operators in the oil and gas industry in boreholes throughout California for information that could indicate stress state or orientation within the upper crust. These well logs are available to students at LSU through a proprietary database of historic industry-collected well logs. Harris searched through ~2500 well logs from California, and of those identified one that contains information from oriented logging tools that could be used to ascertain stress azimuth (SHmax), comparable to the published stress orientations from borehole breakouts documented by *Wilde and Stock* [1997].

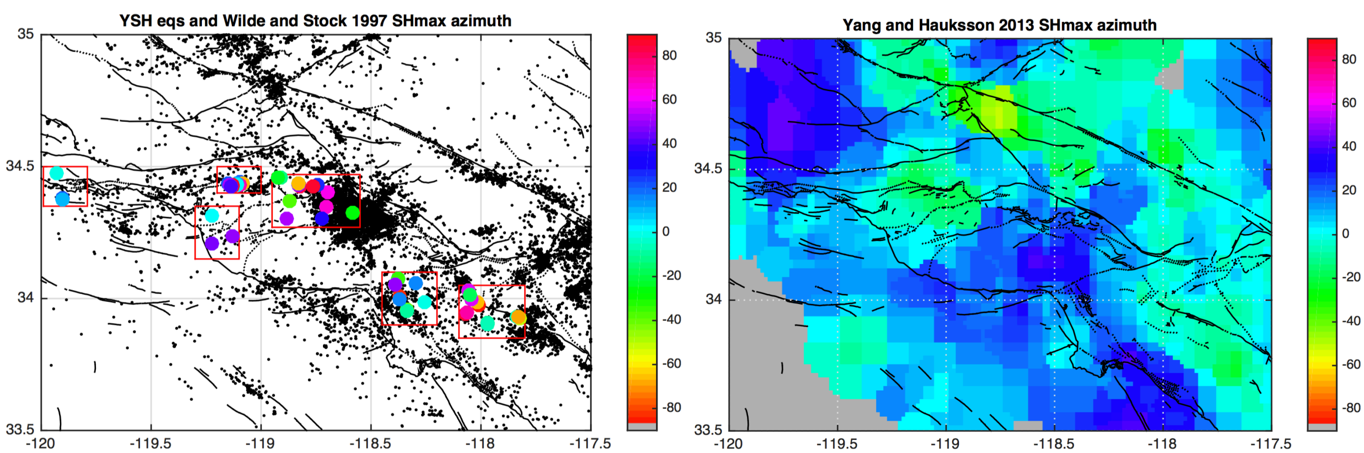

Figure 3: a) earthquake locations in the YSH2010 catalog [*Hauksson et al*., 2012; *Yang et al*., 2012] and SHmax azimuths inferred from borehole breakouts [*Wilde and Stock*, 1997]. b) SHmax azimuth inferred from inversion of YSH2010 catalog with regional smoothing enforced [*Yang and Hauksson*, 2013].

Preliminary investigations comparing such borehole observations and focal mechanism stress inversions [*Yang and Hauksson*, 2013] indicate strong disagreement between the two (Figure 3), primarily due to considerable small-scale heterogeneity present among stress observations derived from borehole breakouts [*Persaud et al*., 2015]. However, the focal mechanism inversion method prioritizes recovering the smoothest possible stress field from a regional-scale inversion. As such, it is inherently insensitive to the local-scale stress variations suggested by borehole observations and incapable of addressing the degree and scale of heterogeneity present within the crustal stress field. Further study will be required to determine whether the two sets of stress observations are truly incompatible, indicating a difference in stress field between near-surface and seismogenic depths, or whether the stress field orientation could possibly be homogeneous with depth throughout the upper crust.

REFERENCES

Behr, W. M., and J. P. Platt (2011), A naturally constrained stress profile through the middle crust in an extensional terrane, *Earth Planet. Sci. Lett.*, *303*(3-4), 181-192, doi:10.1016/j.epsl.2010.11.044.

Brace, W. F., and D. L. Kohlstedt (1980), Limits on Lithospheric Stress Imposed by Laboratory Experiments, *J. Geophys. Res.*, *85*(B11), 6248-6252, doi:10.1029/JB085iB11p06248.

Brudy, M., M. D. Zoback, K. Fuchs, F. Rummel, and J. Baumgärtner (1997), Estimation of the complete stress tensor to 8 km depth in the KTB scientific drill holes: Implications for crustal strength, *J. Geophys. Res.*, *102*(B8), 18453, doi:10.1029/96jb02942.

Dahlen, F. A. (1990), Critical Taper Model of Fold-and-Thrust Belts and Accretionary Wedges, *Ann. Rev. Earth Planet. Sci.*, *18*, 55-99.

Fialko, Y., L. Rivera, and H. Kanamori (2005), Estimate of differential stress in the upper crust from variations in topography and strike along the San Andreas fault, *Geophys. J. Int.*, *160*(2), 527-532.

Hardebeck, J. L., and E. Hauksson (2001), Crustal stress field in southern California and its implications for fault mechanics, *J. Geophys. Res.*, *106*(B10), 21859-21882, doi:10.1029/2001jb000292.

Hardebeck, J. L., and A. J. Michael (2006), Damped regional-scale stress inversions: Methodology and examples for southern California and the Coalinga aftershock sequence, *J. Geophys. Res.*, *111*(B11), doi:10.1029/2005jb004144.

Hauksson, E., W. Yang, and P. M. Shearer (2012), Waveform Relocated Earthquake Catalog for Southern California (1981 to 2011), *Bull. Seismol. Soc Am.*, *102*(5), doi:10.1785/0120120010.

Hickman, S., and M. D. Zoback (2004), Stress orientations and magnitudes in the SAFOD pilot hole, *Geophys. Res. Lett.*, *31*(15), doi:10.1029/2004gl020043.

Hirth, G., C. Teyssier, and J. W. Dunlap (2001), An evaluation of quartzite flow laws based on comparisons between experimentally and naturally deformed rocks, *Int. J. Earth Sciences*, *90*(1), 77-87, doi:10.1007/s005310000152.

Luttrell, K., and D. Sandwell (2012), Constraints on 3-D stress in the crust from support of mid-ocean ridge topography, *J. Geophys. Res.*, *117*(B4), doi:10.1029/2011jb008765.

Luttrell, K., and B. Smith-Konter (2017), Limits on crustal differential stress in southern California from topography and earthquake focal mechanisms, *Geophys. J. Int.*, *in review*.

Luttrell, K., and B. Smith-Konter (2017, manuscript in preparation), Near fault crustal stress in southern California with implications for heterogeneous tectonic loading, *to be submitted to J. Geophys. Res.*

Nicholson, C., A. Plesch, C. Sorlien, J. Shaw, and E. Hauksson (2013), Updating the 3D fault set for the SCEC Community Fault Model (CFM-v4) and revising its associated fault database, *SCEC Annual Meeting*(poster 123).

Persaud, P., J. Stock, and D. Smith (2015), Evidence of sub Kilometer-scale Variability in Stress Directions near Active Faults: An Example from the Newport-Inglewood Fault, Southern California, *American Geophysical Union, Fall Meeting*(abstract T23C-2972).

Plesch, A., et al. (2007), Community fault model (CFM) for southern California, *Bull. Seismol. Soc Am.*, *97*(6), 1793-1802, doi:10.1785/0120050211.

Wilde, M., and J. Stock (1997), Compression directions in southern California (from Santa Barbara to Los Angeles Basin) obtained from borehole breakouts, *J. Geophys. Res.*, *102*(B3), 4969, doi:10.1029/96jb03734.

Yang, W., and E. Hauksson (2013), The tectonic crustal stress field and style of faulting along the Pacific North America Plate boundary in Southern California, *Geophys. J. Int.*, *194*(1), 100-117, doi:10.1093/gji/ggt113.

Yang, W., E. Hauksson, and P. M. Shearer (2012), Computing a Large Refined Catalog of Focal Mechanisms for Southern California (1981-2010): Temporal Stability of the Style of Faulting, *Bull. Seismol. Soc Am.*, *102*(3), 1179-1194, doi:10.1785/0120110311.

Zajac, B., and J. Stock (1997), Using borehole breakouts to constrain the complete stress tensor: Results from the Sijan Deep Drilling Project and offshore Santa Maria Basin, California, *J. Geophys. Res.*, *102*(B5), 10083, doi:10.1029/96jb03914.

Zoback, M. D., and J. H. Healy (1992), In situ stress measurements to 3.5 km depth in the Cajon Pass Scientific Research Borehole: Implications for the mechanics of crustal faulting, *J. Geophys. Res.*, *97*(B4), 5039, doi:10.1029/91jb02175.

Zoback, M. D., S. Hickman, and W. Ellsworth (2010), Scientific Drilling Into the San Andreas Fault Zone, *Eos Trans. AGU*, *91*(22), 197-199, doi:10.1029/2010EO220001.